

Thermodynamic Micellization Model of Asphaltene Precipitation from Petroleum Fluids

Alexey I. Victorov and Abbas Firoozabadi

Reservoir Engineering Research Institute, Palo Alto, CA 94304

A thermodynamic micellization model is proposed for the description of asphaltene precipitation from petroleum fluids. It describes the solubilization of asphaltene polar species by resin bipolar molecules in the micelles. A simple form of the standard Gibbs free energy of micellization is used. The petroleum fluid is assumed to be a dilute solution with respect to the monomeric asphaltenes, resins, and micelles. The Peng–Robinson equation of state (PR-EOS) is applied to describe the fugacity of monomeric asphaltene in the bulk of the petroleum fluid. Intermicellar interactions as well as osmotic pressure effects are neglected. The proposed model shows promising results to describe asphaltene deposition from crude mixtures. It predicts the change in precipitation power of different alkane precipitants and the effect of pressure on asphaltene precipitation. The amount and the onset of predicted asphaltene precipitation are sensitive to the amount of resins in the crude. All these results are in line with laboratory observations and oil-field data.

Introduction

A variety of substances of diverse chemical nature constitute petroleum fluids. These include paraffinic, naphthenic, and aromatic hydrocarbons, and polar polyaromatic materials that contain metals and nitrogen. The polar materials are part of the heavy nonvolatile end of the crude; they are often referred to as “resins,” and “asphaltenes” in petroleum chemistry and petroleum engineering literature (Altgelt and Boduszynski, 1994). Under certain conditions, asphaltenes and resins precipitate from a petroleum fluid (Katz and Beu, 1945; Hirshberg et al., 1984). The precipitation in both underground petroleum reservoirs and production facilities is undesirable. It reduces flow rate and may plug the production facilities.

It is unclear how to exactly define asphaltenes and resins as components with a specific molecular structure. The operational definitions of asphaltenes and resins are based on their solubility in different solvents (Speight, 1980; Hirshberg et al., 1984). Asphaltenes are often defined as the fraction of crude insoluble in normal alkanes such as *n*-pentane and hot *n*-heptane. Resins are assumed to be insoluble in liquid propane but soluble in *n*-pentane. Liquid and gas titration

experiments are performed to determine the amount of solid precipitates. It is believed that titration with low molecular weight alkanes (C_2 to C_4) leads to coprecipitation of both resins and asphaltenes (Leontaritis, 1988). Liquid titration with pentane results in nearly pure asphaltene precipitate. The amount of asphaltene precipitate decreases as the molecular weight of the *n*-alkane titrant increases.

The asphaltenes and resins may associate to form large aggregates of high molecular weights (Lian et al., 1994; Andersen and Speight, 1993; Storm et al., 1991). As early as 1938, it was recognized that asphaltenes and resins form colloid particles (Nellensteyn, 1938). Later, Yen (1974) reconfirmed the formation of micelles in asphaltene and resin-containing crudes. Currently the micellar nature of these systems is a well-established fact (Wiehe and Liang, 1995). On the other hand, asphaltene precipitation modeling has traditionally been approached by using a bulk phase equation of state to describe asphaltene solubility (Hirshberg et al., 1984; James and Mehrotra, 1988; Burke et al., 1990; Kawanaka et al., 1991) neglecting its colloid nature.

A thermodynamic colloid model of asphaltene precipitation was proposed by Leontaritis and Mansoori (1987). This model can be used to assess the possibility of precipitation; however, it does not explicitly deal with the dependence of the micellization process on the characteristics of the mi-

Correspondence concerning this article should be addressed to A. Firoozabadi.
Permanent address of A. I. Victorov: St. Petersburg State University, St. Petersburg, Russia.

celles. A number of advanced thermodynamic models of micellization (Nagarajan and Ruckenstein, 1991; Blankstein et al., 1985; Puvvada and Blankstein, 1992) and colloid stability (Kahlweit and Reiss, 1991; Madahevan and Hall, 1990) have been elaborated in the physicochemical literature, basically for aqueous systems. These models have been applied to protein flocculation (Madahevan and Hall, 1990; Vlachy et al., 1993; Chiew et al., 1995), solubilization (Nagarajan and Ruckenstein, 1991), and related phenomena. The term solubilization was first introduced by McBain and Hutchinson (1955) to denote a pronounced enhancement of the solubility of a material by its sorption in micelles. In this work, we develop a simple thermodynamic model of solubilization of asphaltene material by resins, adopting and modifying the micellization models by Nagarajan and Ruckenstein (1991), Blankstein et al. (1985), Puvvada and Blankstein (1992).

This article begins with a discussion of the thermodynamics of aggregation of asphaltene and resin monomeric species to form colloid particles. Then we present the model for asphaltene precipitation from crudes. Next, the proposed micellization model is applied to describe liquid and gas titration, and to predict the effect of pressure on the stability of a crude with respect to asphaltene precipitation. We conclude the article with some propositions for future work.

Thermodynamics of Micellization

Aggregation equilibrium

We assume that an asphaltene colloid particle has a core, which is formed by n_1 aggregated asphaltene molecules; n_2 bipolar resin molecules are adhered on the surface of the core (Figure 1). The aggregate is called a *micelle*. Several further assumptions are made about the structure of a micelle based on spectroscopic evidence (Espinat and Ravey, 1993;

Speight, 1980). The role of resins is analogous to that which is played by surfactant amphiphilic molecules in theories of solubilization. If not for the resins, we believe, most of the asphaltene material would immediately precipitate from the crude due to a low solubility of asphaltene monomeric molecules in the bulk of the petroleum fluid. The balance between the amount of the asphaltene material solubilized within the micelles and what remains in the form of monomers is governed by the aggregation equilibrium, which can be written (Tanford, 1973; Rusanov, 1992) as

$$\mu_M^\beta = n_1 \mu_{a1}^\beta + n_2 \mu_{r1}^\beta. \quad (1)$$

In the preceding equation, μ_M^β is the chemical potential of a micelle consisting of n_1 asphaltene molecules and n_2 resin molecules, and μ_{a1}^β and μ_{r1}^β are the chemical potentials of monomeric asphaltene and resin molecules, respectively. The medium (petroleum fluid) is noted by index β (Figure 1). Equation 1 determines the distribution of micelles over their sizes (n_1 and n_2), and is valid both for the monodisperse (all the micelles are of the same size) and polydisperse (the diversity of micellar sizes) colloid mixtures. This equation is also valid both for concentrated and for dilute solutions. In our work, it is assumed that the concentrations of resin and asphaltene monomeric species and micelles are small enough to apply thermodynamics of dilute solutions (thus we exclude heavy oils that might be rich in asphaltene and resin content), and therefore we can write:

$$\mu_{a1} = \mu_{a1}^* + kT \ln X_{a1}, \quad (2)$$

$$\mu_{r1} = \mu_{r1}^* + kT \ln X_{r1}, \quad (3)$$

for the monomeric asphaltenes and resins, respectively, and

$$\mu_M = G_M^{00} + kT \ln X_M \quad (4)$$

for the micelles (note that superscript β in these and subsequent equations is dropped). In Eqs. 2–4, X_i is the mole fraction of species i and μ_{a1}^* , μ_{r1}^* , and G_M^{00} are the standard chemical potentials. The standard state is chosen to be that of the petroleum fluid, which is infinitely diluted with respect to “solutes” (monomeric asphaltenes, resins, and micelles). Thus, the standard chemical potential of a solute k , μ_k^* , is defined by the properties of the isolated particle k (a monomer molecule or a micelle) in the solvent (the petroleum fluid free of asphaltene and resin monomers and micelles),

$$\mu_k^* = \lim_{\sum X_s \rightarrow 0} (\mu_k - kT \ln X_k), \quad (5)$$

where the summation extends over different solutes (Prigogine and Defay, 1952). In a dilute solution, the difference between these standard free energies determines the distribution of micelles over their size and composition. As it can readily be seen by rewriting the condition of aggregation equilibrium, Eq. 1, and Eqs. 2–4 to give:

$$X_M = \exp\{(n_1 \mu_{a1} + n_2 \mu_{r1} - G_M^{00})/kT\}, \quad (6)$$

or

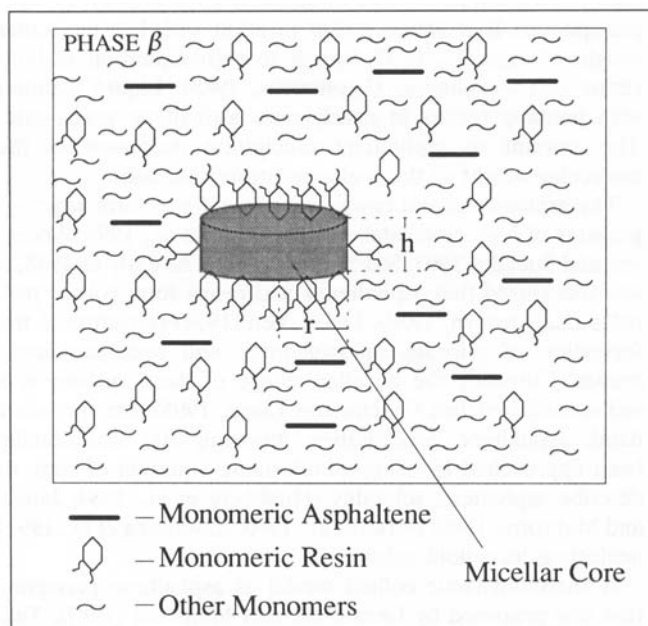


Figure 1. Micelles, monomeric asphaltenes, and resins in a petroleum fluid medium.

$$X_M = X_{a1}^{n_1} X_{r1}^{n_2} \exp\{\Delta G_M^{00}/kT\}, \quad (7)$$

with the standard Gibbs energy of the formation of a micelle (micellization), ΔG_M^{00} , defined by

$$\Delta G_M^{00} = n_1 \mu_{a1}^* + n_2 \mu_{r1}^* - G_M^{00}. \quad (8)$$

A model for the Gibbs energy of micellization should take into account the micellar size, shape, composition, and should include various contributions to the micellization process. We will formulate such a model later in this article.

Material balance

In addition to the aggregation equilibrium, one also has to consider the material balance. Prior to the precipitation of the asphaltene material,

$$\begin{aligned} N_a &= N_{a1} + \sum_{n_1, n_2}^{\infty} n_1 N_M(n_1, n_2), \\ N_r &= N_{r1} + \sum_{n_1, n_2}^{\infty} n_2 N_M(n_1, n_2), \end{aligned} \quad (9)$$

where N_a and N_r are the gross numbers of asphaltene and resin molecules in the crude, N_{a1} and N_{r1} are the numbers of asphaltene and resin monomeric species, and $N_M(n_1, n_2)$ is the number of micelles containing n_1 asphaltene molecules and n_2 resin molecules each. The summation is performed over all possible aggregation numbers n_1 and n_2 . With the precipitation of the asphaltene phase, the material balance equations should include the amount of the precipitate. If the precipitate (phase γ) contains only pure asphaltene material, the first of the preceding equations takes the form:

$$N_a = N_a^\gamma + \left[N_{a1} + \sum_{n_1, n_2}^{\infty} n_1 N_M(n_1, n_2) \right], \quad (10)$$

and the second one remains intact.

At a given temperature, pressure, and given gross composition, Eq. 9 together with Eq. 7 determine the micellar–monomer equilibrium and the distribution of the aggregates over their size and composition. These equations may be difficult to solve, since they contain a very large number of unknowns, $N_M(n_1, n_2)$. If the distribution of the micelles were sharp both with respect to their composition and with respect to their size, we could approximate their distribution by the most probable terms, and write instead of Eq. 9:

$$N_a = N_{a1} + n_1^0 N_M(n_1^0, n_2^0) \quad (11a)$$

$$N_r = N_{r1} + n_2^0 N_M(n_1^0, n_2^0), \quad (11b)$$

with the corresponding values of $n_1 = n_1^0$ and $n_2 = n_2^0$, which represent the micelles that are most probable to form. The assumption that all the micelles are of the same size can be justified in the case of small colloid particles of spherical shape (Nagarajan and Ruckenstein, 1991; Puvvada and Blankstein, 1992). For large platelike aggregates, one would

expect polydispersity. In this article, we assume that all the micelles are monodispersed. This assumption is made for the sake of computational simplicity and in principle can be removed.

Gibbs free energy of micellization

All the specific features of the micellization model (micellar structure and molecular characteristics) are contained in the standard Gibbs energy term. According to Nagarajan and Ruckenstein (1991) and Puvvada and Blankstein (1992), there are several major contributions in the process of micelle formation in a dilute solution.

(a) *Lyophobic Contributions.* The lyophobic contribution to ΔG_M^{00} represents the free-energy gain upon transferring asphaltene and resin molecules from an infinitely diluted crude to a micelle. We shall relate this term with the solubility of asphaltene in the bulk of the crude at the onset of asphaltene precipitation. Suppose that the pure solid asphaltene phase (γ) is in equilibrium with the micellar crude solution (phase β), then the chemical potential of the solid asphaltene, and asphaltene monomers in liquid phase are equal:

$$\mu_a^\gamma(T, P) = \mu_{a1}^\beta = \mu_{a1}^* + kT \ln X_{a1}^\beta. \quad (12)$$

Here $X_{a1}^\beta \equiv X_{a1}^{\text{ons}}$ is the equilibrium concentration of monomeric asphaltenes in the crude coexisting with the solid asphaltene phase. Under the assumption that the average state of an asphaltene molecule in the micellar core (more precisely, in a hypothetical uniform state, corresponding to a micellar core at the pressure P^β , Rusanov (1992)) is similar to its state in the solid asphaltene phase, one can write:

$$\mu_a^{\text{Mic.core}}(T, P^\beta) - \mu_{a1}^* \approx \mu_a^\gamma(T, P^\beta) - \mu_{a1}^* = kT \ln X_{a1}^{\text{ons}}, \quad (13)$$

which is the contribution to the micellization “lyophobic term” due to the transfer of an asphaltene molecule. Since the solubility of asphaltene monomers in the crude is low, the right-hand side of Eq. 13 is substantially negative, and thus the lyophobic effect essentially enhances the solubilization of asphaltenes in the micelles (Nagarajan and Ruckenstein, 1991). It is this term that makes the aggregated state preferable over the monomeric state. Equation 13 is the essence of our phenomenologic micellization model and is similar to that of Tanford (1973), which we apply here to the solid–liquid equilibrium. The quantity X_{a1}^{ons} will be our main parameter. It reflects how much monomeric asphaltene a crude can hold.

Another contribution to the “lyophobic term” is due to the transfer of a resin molecule from a dilute crude onto an asphaltene micellar core. The transfer is associated with breaking the resin–crude interactions and creating resin–asphaltene and resin–resin interactions. This process can be considered as adsorption of resins from the petroleum fluid on asphaltene aggregates. A simple way of expressing the free-energy change upon the transfer of a single resin molecule is to write purely energetic (ΔU_r) and purely entropic (ΔS_r) terms as

$$\Delta U_r = a(\bar{U}_{r-c} - \bar{U}_{r-a}),$$

$$\Delta S_r = -k \ln[1 - A_r(n_2)/A_\Sigma]. \quad (14)$$

In Eq. 14, a is the surface area of a resin molecule polar head, \bar{U}_{r-c} and \bar{U}_{r-a} are the average interaction energies of the resin molecule head with the crude and with asphaltene molecules (micellar core), respectively, A_Σ is the total surface area of a micelle, and $A_r(n_2)$ is the surface area occupied by n_2 resin molecules. Since polar resin heads associate with asphaltenes, the ΔU_r term is positive. As a first approximation, ΔU_r is considered to have some properly averaged value, which remains the same for a given petroleum fluid at a given temperature, and does not change appreciably upon the addition of a precipitant, as long as the system remains diluted with respect to resins. This rough approximation may be refined by a more detailed molecular consideration of ΔU_r in future studies.

The ΔS_r term is determined by the probability for a resin molecule to find an unoccupied space to be accommodated on the micellar surface (excluded surface area, repulsion component of the two-dimensional pressure; Puvvada and Blankstein (1992)). This term always opposes micellization, giving a negative contribution to ΔG_M^{00} .

Apart from the lyophobic contribution, other terms determining the free energy of micellization include the following.

(b) *Interfacial Contribution.* A definite positive interfacial tension might be attributed to the micellar core in the crude. The adsorption of bipolar resins on the micellar core surface is likely to lower the interfacial tension ("interfacial screening effect," Nagarajan and Ruckenstein, 1991; Puvvada and Blankstein, 1992), and to contribute to the colloid stability. Kahlweit and Reiss (1991) have shown that this effect alone can explain the stability of a microemulsion. The interfacial term can be written as,

$$\sigma A_\Sigma = \sigma_0[A_\Sigma - A_r(n_2)] + \sigma_s A_r(n_2), \quad (15)$$

where σ is the true interfacial tension between a micelle and the petroleum fluid, σ_0 is the interfacial tension at zero adsorption of resins onto a micelle, and σ_s is the interfacial tension at an interface fully saturated by resins. We assume that resins are surface active with respect to micelles, and that $\sigma_s \approx 0$ (Puvvada and Blankstein, 1992; Kahlweit and Reiss, 1991). Thus Eq. 15 becomes (see Appendix A),

$$\sigma A_\Sigma = \sigma_0[A_\Sigma - A_r(n_2)]. \quad (16)$$

Until now we have not considered the micellar shape. However, A_Σ and $A_r(n_2)$ can be expressed in terms of micellar size and geometric characteristics of asphaltene and resin molecules for a given micellar shape. We use the platelike model of a micelle (Figure 1), a popular point of view (Speight, 1980), which is in agreement with the spectroscopic measurements by Espinat and Ravey (1993). Denoting by n_2^s the maximum number of the resin molecules (heads), which can be accommodated on the flat surfaces of a micellar core, we express the micellar core radius, r , and the micellar core thickness, h , as

$$r = (an_2^s/2\pi)^{1/2}, \quad (17)$$

$$h = v_a n_1 / \pi r^2, \quad (18)$$

where v_a is the asphaltene molecular volume. Equation 16 then becomes

$$\sigma A_\Sigma = \sigma_0 \left[n_1 v_a \left(\frac{8\pi}{an_2^s} \right)^{1/2} + (n_2^s - n_2) a \right]. \quad (19)$$

(c) *Electrostatic Contribution.* Electrostatic effects may accompany the micellization in highly aromatic crudes where the charged particles can be stabilized. It is unlikely, however, that these effects can govern the process of micelle formation in a typically dielectric medium such as a petroleum fluid. In this work, we are concerned with only those ΔG_M^{00} contributions that seem crucial for colloid stability, and electrostatic effects are neglected.

To summarize, we write the final expression for the Gibbs energy of micellization as

$$\Delta G_M^{00} = n_1(\mu_{a1}^* - \mu_a^M) + n_2(\mu_{r1}^* - \mu_r^M) - \sigma A_\Sigma, \quad (20)$$

where

$$\mu_{a1}^* - \mu_a^M = -kT \ln X_{a1}^{\text{ons}}, \quad (21)$$

$$\mu_{r1}^* - \mu_r^M = \Delta U_r - T\Delta S_r, \quad (22)$$

and μ_a^M , μ_r^M are the chemical potentials of asphaltene and resin molecules in a hypothetical uniform micellar phase at pressure P^β of the surrounding petroleum fluid and σA_Σ is defined by Eq. 19. Introducing $\Theta = A_r(n_2)/A_\Sigma$, the fraction of micellar core surface covered by resins, we can rewrite Eq. 20 as

$$\frac{\Delta G_M^{00}}{RT} = n_2 f(\Theta) - n_1 \ln X_{a1}^{\text{ons}}, \quad (23)$$

where

$$f(\Theta) = \ln(1 - \Theta) + \frac{\Delta U_r}{RT} - \frac{\sigma_0 a(1 - \Theta)}{RT\Theta}, \quad (24)$$

Equations 23 and 24 are essentially our micellization model. These two equations combined with the aggregation equilibrium equation (Eq. 7) and material balance relations determine the micellar-monomer equilibrium.

Micellar size and composition distribution

Equation 7 determines the concentration of micelles as a function of aggregation numbers n_1 and n_2 for given concentrations of monomeric asphaltenes and resins. It should suffice then to determine what kind of micelles (of what size and what composition) are most probable to form at a given state of the crude. We expect that the distribution over the various micellar compositions (or, equivalently, coverages Θ) is narrow enough (Puvvada and Blankstein, 1992) to represent the whole population of micelles by those having the optimum composition. We consider monodisperse micelles,

not only because the problem is simplified, as was stated earlier, but also because it is unlikely that the account of the polydispersity could significantly change the model's ability to explain the phenomenon of asphaltene precipitation. The optimum composition of a micelle of a given size, $n = n_1 + n_2$, is determined by

$$\left(\frac{\partial \ln X_M}{\partial \Theta} \right)_n = 0, \quad (25)$$

which, by virtue of Eqs. 7, 23, and 24, becomes (see Appendix A)

$$\ln \left(\frac{X_{a1}}{X_{r1} X_{a1}^{\text{ons}}} \right) - \frac{\Delta U_r}{RT} - \frac{\sigma_0 a}{RT} (1 + b) = \ln(1 - \Theta) - \frac{\Theta}{(1 - \Theta)} (1 + \Theta b), \quad (26)$$

where

$$b = \frac{v_a}{a} \left(\frac{8\pi}{an_2^2} \right)^{1/2} \quad (27)$$

is determined by the geometrical characteristics of the asphaltene and resin molecules and by micellar radius. Equation 26 determines the most probable composition of a micelle, Θ , provided the total aggregation number, n is given.

Micellization model parameters

The parameters that determine the micellization process have "molecular" meaning and, in principle, can be estimated or regressed from experimental data. The parameters are:

- $\Delta U_r/RT$ characterizes the difference between the interaction energy of a resin molecule head with the petroleum medium and the interaction energy of the resin molecule head with asphaltenes in a micellar core. This parameter correlates with the heat of adsorption of resins on solid asphaltenes, but unfortunately there are no relevant data in the literature. The value of this parameter was guessed by some preliminary calculations of asphaltene micellization for a model crude and was kept constant for all the crudes considered in this work.

- $\sigma_0 a/RT$ characterizes the interfacial tension between the asphaltene micellar core and the crude. To our knowledge, there is no direct experimental measurement of this parameter either. We also guessed this parameter and kept it constant for all the crudes (to be presented later in the results section).

- b is the "molecular" geometrical parameter (Eq. 27) that is related to n_2^2 (or, equivalently, the micellar radius, r , see Eq. 17). For a given micellar radius, parameters b and n_2^2 can be estimated from the knowledge of the resin molecule head's specific surface area, a , and the solid asphaltene specific volume, v_a (Eqs. 17 and 27). There are no direct experimental measurements of a and v_a . However, a reasonable estimate of their magnitude can be made. The spectroscopic data on micellar radius, thickness, and the estimates of the aggregation numbers are available (Espinat and Ravey, 1993; Storm and Sheu, 1993, 1994).

- X_{a1}^{ons} is the concentration of asphaltene monomers in the crude in equilibrium with the pure solid asphaltene phase. It is the maximum concentration of monomeric asphaltenes in a crude at given conditions. This quantity is a characteristic of a given crude, and is adjusted from experimental data on asphaltene deposition for each individual crude mixture.

- n is the micellar size for the "monodispersed" model. Its value was chosen to a large extent arbitrarily, just to ensure that stable micelles are present in the crude, and that their size is in line with the spectroscopic data. The sensitivity of the model to n was also examined. In principle, this parameter can be removed, as discussed earlier.

Incorporation of the Equation of State

An equation of state can be used to express the chemical potential of all the monomers in the crude. In this manner, the effect of pressure, temperature, and composition of the petroleum fluid can be taken into account. Since the main contribution to the micellization Gibbs free energy is the "lyophobic term," Eq. 13, let us start with the consideration of its EOS-dependence, leaving all the other contributions intact. This is equivalent to saying that the bulk asphaltene solubility determines the asphaltene precipitation process, through the formation and destruction of the micelles. The quantity X_{a1}^{ons} changes by adding a solvent or changing the pressure along the equilibrium solid-fluid line:

$$d\mu_a^\gamma(T, P) = d[\mu_{a1}^*(T, P, \mathbf{x}^*) + kT \ln X_{a1}^{\text{ons}}], \quad (28)$$

where $\mu_{a1}^*(T, P, \mathbf{x}^*)$ is the standard chemical potential of monomeric asphaltene, and \mathbf{x}^* denotes the composition of the "solvent" (petroleum fluid diluted with respect to asphaltenes, resins, and micelles). Any conventional bulk EOS can be used to estimate $d\mu_{a1}(T, P, \mathbf{x})$. Even the extreme polarity of asphaltene molecules does not matter anymore, since the solution is dilute. In the present work, the Peng-Robinson equation of state (PR-EOS, Peng and Robinson, 1976) is used.

Solvent influence

In the liquid titration experiments an asphaltene precipitant (an alkane) is added to a crude oil at a constant temperature and pressure. For such a process,

$$d[\mu_{a1}^*(T, P, \mathbf{x}^*) + kT \ln X_{a1}^{\text{ons}}] = 0, \quad (29)$$

which upon expressing the standard chemical potential by an EOS and integration, gives

$$X_{a1}^{\text{ons}}(T, P, \text{ratio}) = X_{a1}^{\text{ons}}(T, P, \text{ratio} = 0) \frac{\varphi_{a1}^\beta(T, P, \text{ratio} = 0)}{\varphi_{a1}^\beta(T, P, \text{ratio})}, \quad (30)$$

where φ_{a1}^β is the fugacity coefficient of monomeric asphaltene species in the petroleum fluid medium, given by a bulk phase equation of state, and "ratio" is the dilution ratio, a compositional variable used normally in liquid titration experiments, which is defined as the added volume of solvent

divided by the amount of the original crude; ratio = 0 denotes the original state before dilution. According to Eq. 30, the micellization parameter, $X_{a1}^{ons}(T, P, \text{ratio})$ is related to the fugacity of the monomeric asphaltene species calculated from the EOS. Note that this quantity depends both on the amount of the added solvent (i.e., ratio) and the type of the solvent (i.e., pentane, heptane, etc.). $X_{a1}^{ons}(T, P, \text{ratio} = 0)$ has, of course, the same value for different solvents and is the characteristic of the particular crude mixture.

Pressure influence

Similar considerations can be applied to estimate the effects of pressure on X_{a1}^{ons} . We integrate Eq. 28 from the initial pressure P to the final pressure P' . Assuming that solid asphaltene is incompressible, and that it has the same molecular volume as in the micellar core, we get:

$$X_{a1}^{ons}(P') = X_{a1}^{ons}(P) \frac{\varphi_{a1}^{\beta}(T, P, \mathbf{x})P}{\varphi_{a1}^{\beta}(T, P', \mathbf{x}')P'} \exp\left(\frac{v_a(P' - P)}{RT}\right), \quad (31)$$

where $X_{a1}^{ons}(P')$ is the monomeric asphaltene concentration at pressure P' , and \mathbf{x}' is the composition at P' . Upon differentiation,

$$\left(\frac{\partial X_{a1}^{ons}}{\partial P'}\right)_{T, \mathbf{x}'} = X_{a1}^{ons}(P') \left[\frac{v_a}{RT} - \frac{1}{\varphi_{a1}^{\beta}(T, P', \mathbf{x}')} \left(\frac{\partial \varphi_{a1}^{\beta}(T, P', \mathbf{x}')}{\partial P'} \right)_{T, \mathbf{x}'} - \frac{1}{P} \right]. \quad (32)$$

The lefthand side of Eq. 32 is positive at moderate and high pressures provided that the derivative of the fugacity coefficient

of monomeric asphaltene is negative. This means that lowering the pressure will lower X_{a1}^{ons} , and therefore the ability of the crude to carry asphaltene material reduces at lower pressures. In other words, we would expect the asphaltene material to precipitate by depressurizing the crude, which is in agreement with experimental observations (Hirshberg et al., 1984; Burke et al., 1990). However, Eq. 32 also implies that at certain conditions, we might expect the opposite behavior. At high temperatures and low pressures, pressurizing a mixture will cause precipitation if the derivative in the lefthand side of Eq. 32 becomes negative.

Calculation Results

Prior to the presentation of results, we will briefly outline the calculation procedure. For a given temperature, pressure, and gross composition, there are five unknowns X_{a1} , X_{r1} , X_M , n_1 , and n_2 . There are also five equations, Eqs. 7, 11a, 11b, and 26, and $n = n_1 + n_2$; n , X_{a1}^{ons} , and the micellization model parameters are provided. With the initial guess for X_{a1} and X_{r1} , Eq. 26 is solved for micellar size, Θ . From $n = n_1 + n_2$ and $\Theta = n_2/[n_1b + n_2^s]$, n_1 and n_2 are obtained and Eq. 23 is used to calculate ΔG_M^{00} . The mole fraction of micelles can be calculated from Eq. 7, and updated X_{a1} , X_{r1} are obtained from the material balance equations, Eqs. 11a and 11b, until convergence. If $X_{a1}^{\beta} < X_{a1}^{ons}$, the asphaltene phase would not precipitate; otherwise, there would be precipitation and the amount can be calculated from Eq. 10. Note that X_{a1}^{ons} in Eq. 26 should be either obtained from Eq. 30 or Eq. 31.

The preceding model has been applied to describe asphaltene precipitation in liquid (Hirshberg et al., 1984) and gas titration experiments (Burke et al., 1990), and upon depressurizing of a live oil (Hirshberg et al., 1984; Burke et al., 1990). The composition of the crudes studied was obtained by a standard characterization procedure (see Appendix B) and is given in Table 1. The contribution of the osmotic pressure

Table 1. Petroleum Fluid Mixtures and the Gas Mixture Used in the Titration Experiments

Component	Fluid number*									
	1		2		3		4		5	
	mol %	mol wt.	mol %	mol wt.	mol %	mol wt.	mol %	mol wt.	mol %	
N ₂	—	—	—	—	0.57	—	0.51	—	3.17	
CO ₂	—	—	—	—	2.46	—	1.42	—	17.76	
C ₁	0.10	—	0.07	—	36.37	—	6.04	—	30.33	
C ₂	0.48	—	0.07	—	3.47	—	7.00	—	26.92	
C ₃	2.05	—	0.87	—	4.05	—	6.86	—	13.09	
i-C ₄	0.88	—	0.53	—	0.59	—	0.83	—	1.26	
n-C ₄	3.16	—	2.44	—	1.34	—	3.35	—	4.66	
i-C ₅	1.93	—	1.71	—	0.74	—	0.70	—	0.77	
n-C ₅	2.58	—	2.36	—	0.83	—	3.46	—	1.26	
C ₆	4.32	—	4.32	—	1.62	—	3.16	—	0.78	
C ₇	—	—	—	—	—	—	—	—	—	
ps-1	47.45	151.7	24.00	133.5	18.20	142.0	16.67	130.5	—	
ps-2	24.84	239.3	23.00	171.0	13.98	274.0	17.77	222.0	—	
ps-3	5.46	669.4	23.83	230.3	3.69	350.9	20.58	276.9	—	
ps-4	—	—	12.75	340.0	—	—	3.79	430.0	—	
ps-5	—	—	2.069	693.7	—	—	—	—	—	
resin	5.73	603.0	1.836	603.0	8.93	603.0	5.80	603.0	—	
asphalt	1.02	850.0	0.145	850.0	3.17	850.0	2.06	850.0	—	

* These numbers correspond to the following mixtures from the original works: 1 = Hirshberg et al., 1984, tank oil No. 1; 2 = Hirshberg et al., 1984, tank oil No. 2; 3 = Burke et al., 1990, live oil No. 1; 4 = Burke et al., 1990, live oil No. 2; 5 = Burke et al., 1990, gas solvent used in the gas titration experiment.

(Mahadevan and Hall, 1990) due to the presence of micelles was neglected. Somewhat arbitrarily, we assigned the molecular weights of the monomeric asphaltenes and resins, and kept them the same for all the mixtures (Table 1). The asphaltene molar volume was estimated as $v_a = 0.5 \text{ m}^3/\text{kmol}$. The resin molecule polar head surface area was taken to be $a = 40 \text{ \AA}^2$, close to the surface area reported by Nagarajan and Ruckenstein (1991) for alkyl glucoside polar head group. The interfacial tension between a polar asphaltene micellar core and apolar crude is supposed to be large, and we set it to be $\sigma_0 = 0.040 \text{ N/m}$. After some preliminary calculations, the resins adsorption energy was chosen to be $(\bar{U}_{r-c} - \bar{U}_{r-a}) = 0.073 \text{ J/(mol} \cdot \text{m}^2)$. This value ensures the possibility of the existence of stable micelles and corresponds to a molar adsorption energy of approximately 18 kJ/mol , a value that seems reasonable for the adsorption of a polar aromatic resin group onto asphaltene solid core.

There is an element of arbitrariness in assigning the model parameter values, due to a lack of the experimental information. As an example, there are no data on σ_0 , a , or $(\bar{U}_{r-c} - \bar{U}_{r-a})$. There is also uncertainty in the characterization of real petroleum fluids, leaving doubts about the mole fractions of the components, which are the input in our model. This makes questionable an explicit proof of the model validity. Our major goal is, therefore, to show that with some reasonable values assigned to the parameters, the model would describe the main features of asphaltene precipitation from crudes. In our calculations, X_{a1}^{ons} is adjusted individually for every petroleum fluid mixture while other parameters are kept constant.

Liquid titration

For the liquid titration experiments the amount of resin is estimated to be the difference between the reported amount of asphalt and asphaltene material in the crude (Hirshberg et al., 1984). The quantity X_{a1}^{ons} is obtained by adjusting the calculated amount of asphaltene precipitated by *n*-decane. We found $X_{a1}^{\text{ons}} = 2.4 \times 10^{-3}$ mole fraction for tank oil 1 (Table 1) assuming monodispersed micelles with $n = 250$ and $n_2^s = 200$.

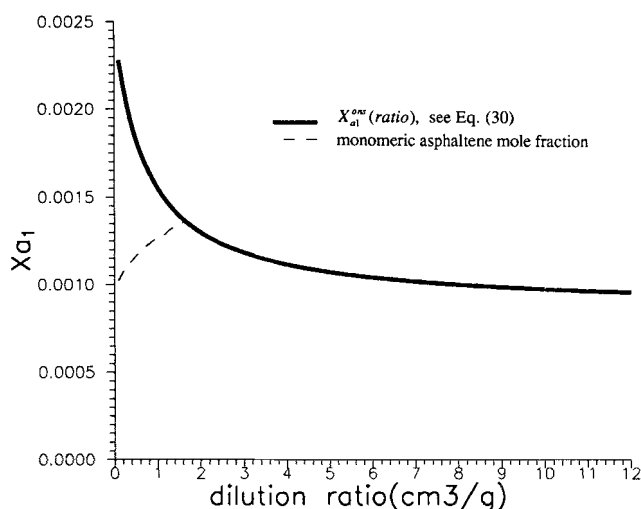


Figure 2. Dilution diagram for tank oil 1 (Table 1) with *n*-decane as a precipitant at 295 K.

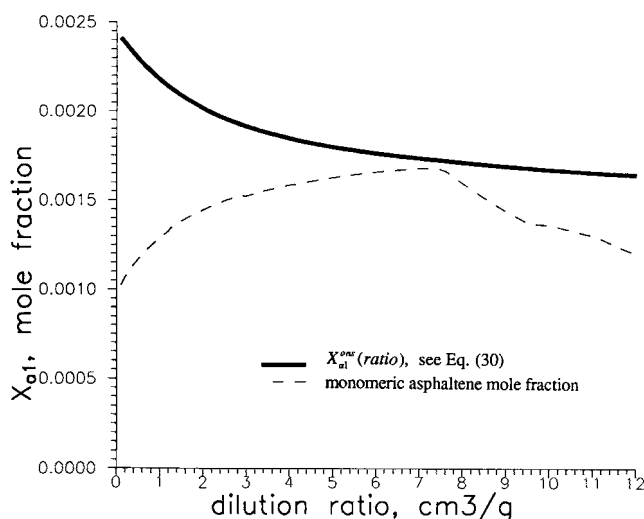


Figure 3. Dilution diagram for tank oil 1 (Table 1) with *n*-octadecane as a precipitant at 295 K.

Figures 2 and 3 illustrate the process of precipitation in terms of monomer–micellar equilibrium. If there were no micelles, the chemical potential of the asphaltene monomers, Eq. 2, would only decrease upon the addition of solvent (due to the decrease of the asphaltene mole fraction). In this case, the crude either expels the asphaltene material originally, or becomes even less likely to form precipitate when diluted. In the case of monomer–micellar equilibrium, however, the addition of a solvent destroys the micelles, and the concentration of monomeric asphaltenes grows (Figures 2 and 3), and so does the chemical potential of monomeric asphaltene species in the petroleum medium. At the same time, the quantity $X_{a1}^{\text{ons}}(T, P, \text{ratio})$, which is given by Eq. 30, decreases (Figures 2 and 3). When the concentration of monomers in the petroleum fluid equals $X_{a1}^{\text{ons}}(T, P, \text{ratio})$ (the intersection of the solid and dashed curves in Figure 2), the asphaltene begins to precipitate. Starting from this dilution ratio, Eq. 28 determines the amount of precipitated asphaltene phase. As the concentration of monomeric asphaltenes in the petroleum medium becomes very small (at high dilution ratios), part of the solid asphaltene material may dissolve back into the crude. However, since this phenomenon has not been observed experimentally (Hirshberg et al., 1984), we did not consider this process. Note that in Figure 3, the addition of *n*-octadecane to the crude decreases the monomeric asphaltene fugacity too little to result in asphaltene precipitation.

The calculated characteristics of the micelles formed in the crude are in agreement with the spectroscopic studies. The core radius is determined by the values assigned to a and to n_2^s ; $r = 35.7 \text{ \AA}$ (Storm and Sheu (1994), give 50–100 \AA as an estimate of the micellar diameter); the optimum composition corresponds to 42 asphaltene molecules and 208 resin molecules per micelle (solubilization ratio $n_1/n_2 = 0.20$), which gives the apparent molecular weight of a micelle of about 160,000 [49,700–136,800 according to Espinat and Ravey (1993), and 100,000 given by Storm and Sheu (1994)]. The micellar core thickness is $h = 8.7 \text{ \AA}$ [its spectroscopic estimate is 6–10 \AA ; Espinat and Ravey (1993)].

At higher dilution ratios the micelles become bigger (which has been observed experimentally upon adding heptane to

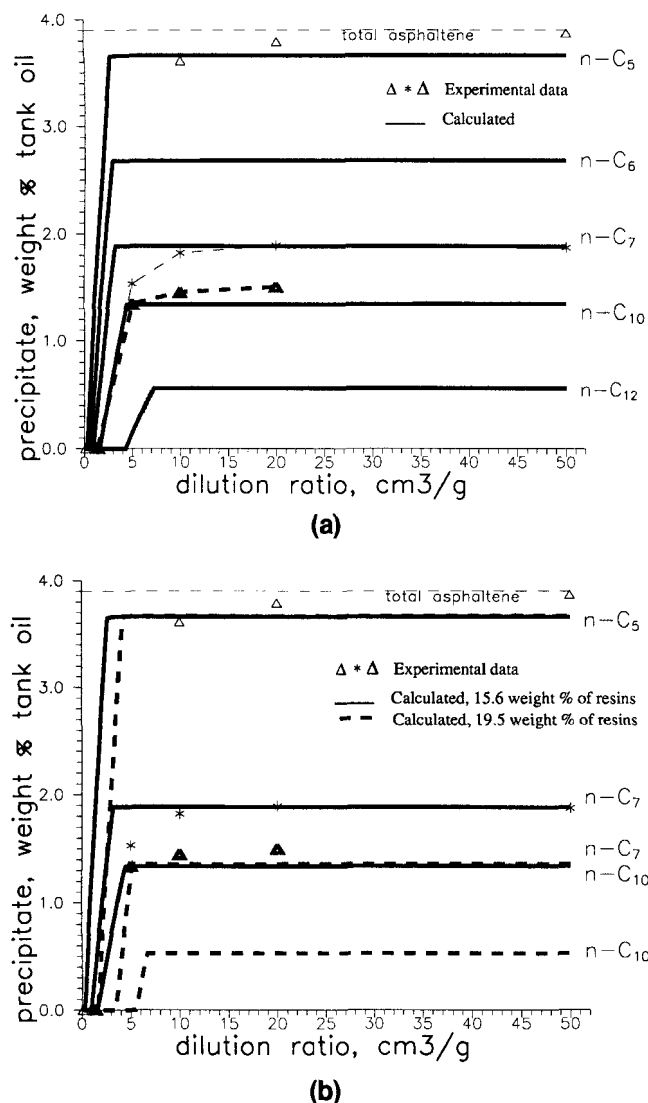


Figure 4. (a) Liquid titration precipitation curves for tank oil 1 (Table 1) at 295 K; (b) effect of resin content on the predicted precipitation curves for tank oil 1 (Table 1) at 295 K.

asphaltene suspended in toluene; Espinat and Ravey (1993)), and then the critical micelle concentration (CMC; Tanford, 1973; Rusanov, 1992) is reached (for decane at a dilution ratio of about 4.6 cm³/g). At CMC, the solubilization ratio is 0.21 and $h = 9.0$ Å. Beyond this dilution ratio, the asphaltene precipitation is determined by the bulk phase thermodynamics, which is the dilute solution–pure solid equilibrium.

The resulting precipitation curves for tank oil 1 with various precipitants are shown in Figure 4a. The model gives the onsets of precipitation and amounts of asphaltene precipitate for different *n*-alkanes added to this crude. It predicts that the precipitation ability of *n*-alkanes decreases with their chain length, so that *n*-heptane, for example, precipitates more asphaltene material than *n*-decane, whereas long-chain alkanes (octadecane, and higher) do not result in precipitation. The amount of the asphaltene precipitated by different alkanes agrees well with the experimental data. Very important is that the predicted amount of asphaltene precipitated

with *n*-pentane is in accord with the operational definition of asphaltene (Figure 4a). This fact was by no means built into our model in advance and thus might be considered as a strong argument for the model validation.

Effect of micellization parameters

We have already stated that several assumptions have been made in model derivation and for model parameters that should be verified, or at least the sensitivity of the calculated results to these assumptions should be examined.

One of the assumptions of our model is monodispersity. We have studied the sensitivity of the calculated results to the aggregation number, *n*, in the range between 100 and 2,000. The calculations performed for *n*-decane titration show a strong dependence of the onset on the micellar size. Small micelles are originally unstable in the crude, and would precipitate without addition of a diluent, while big micelles remain more stable than the solid phase until higher dilution ratios. However, CMC is nearly the same, and so is the total amount of the precipitated solid. As a result, the slope of the precipitation curves is steeper for bigger micelles. Probably the polydispersity of micelles is important for quantitative predictions, and it may be a useful next step for the future development of the model.

The results are also strongly dependent upon the amount of resins present in the crude. Depending on the resin content, a crude may be originally unstable or reveal no precipitation until very high dilution ratios. Figure 4b demonstrates the sensitivity of precipitation to the resin content of the oil. Calculation results based on resin contents of 15.6 and 19.5 wt. % for three precipitants—*n*-C₅, *n*-C₇, and *n*-C₁₀—show that as the resin content of tank oil 1 increases, a higher dilution ratio is required for the onset of precipitation. However, for precipitants that can expell all the asphaltene material from the crude, there are always some high dilution ratios to ensure that all of the asphaltene drops out, no matter what the initial concentration of resins is. In fact, all the characteristics of a crude that affect the mole fractions of resins and asphaltenes have a strong effect on the calculated results, since the mole fractions determine the aggregation equilibrium, Eq. 7. Good estimates of the monomers' molecular weight are important to reliably predict the asphaltene precipitation. Therefore a detailed characterization of the crude heavy end, which is usually not important for vapor–liquid equilibrium calculations, is indispensable for asphaltene precipitation modeling.

The molecular geometry characteristics of resins and asphaltenes and micellization free energy parameters also strongly affect the behavior of a crude. The increase of the resin molecule head surface area, *a*, increases crude stability. For the decane titration of tank oil 1, $a = 35$ Å² leads to the initial instability and precipitation of 2.4 wt. % of asphaltene material, whereas $a = 45$ Å² results in no precipitation at all. The asphaltene molecular volume affects the onset, but not the amount of the precipitated material; the crude is more stable for smaller v_a (it is originally unstable for a volume of about 0.65 m³/kmol and higher).

Parameters σ_0 and $(\bar{U}_{r-c} - \bar{U}_{r-a})$ also play an important role in the micellization process. Lowering σ_0 , as it might be expected, increases stability of the aggregate. For the decane

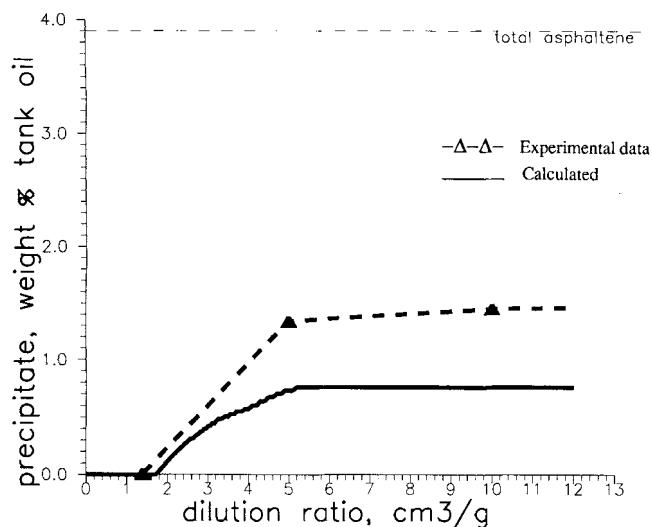


Figure 5. Sensitivity of the predicted precipitation curve of tank oil 1 (Table 1) with *n*-decane to concentration dependent ΔU_r .

titration of Hirshberg et al. (1984), there is no precipitation with $\sigma_0 = 0.01$ N/m; for $\sigma_0 = 0.06$ N/m, the crude is originally unstable and precipitates 2.2 wt. % asphaltene phase. The increase of the $(\bar{U}_{r-c} - U_{r-a})$ parameter to 0.078 J/(mol·m²) shifts the onset to ratio = 7.4 cm³/g and gives 0.1 wt. % precipitated amount of asphaltene for the titration with decane. At $(\bar{U}_{r-c} - U_{r-a}) = 0.079$ J/(mol·m²) there is no precipitation with any amount of decane. We assumed that $(\bar{U}_{r-c} - U_{r-a})$ remains constant, as the crude is diluted with *n*-alkanes. However, the difference between the resin-asphaltene and resin-crude interactions is most likely to grow, as we increase the amount of *n*-alkanes, and the crude becomes more and more apolar. A proper model for the concentration dependence of $(\bar{U}_{r-c} - U_{r-a})$ should be obtained by statistical-mechanical considerations, but in the present study we merely examine the importance of this dependency. Let's assume a

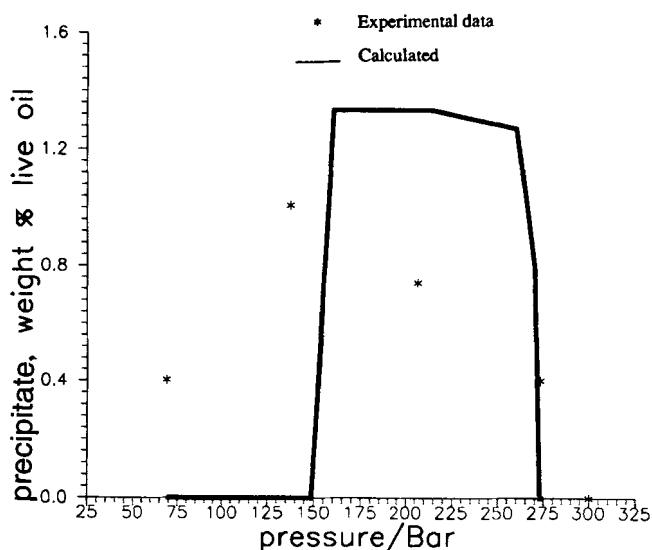


Figure 6. Effect of pressure on precipitation curve for live oil 3 (Table 1) at 373 K.

weak linear dependence of $(\bar{U}_{r-c} - U_{r-a})$ on the dilution ratio—the simplest possible form of a concentration dependence— $(\bar{U}_{r-c} - U_{r-a}) = \text{const.} + 0.00001 \cdot \text{ratio}$. Figure 5 shows the results for decane titration. As can be seen, even a very weak concentration dependency changes the shape of the precipitation curve. The amount of the precipitate is also affected.

The most important contribution to the standard micellization free energy is due to the X_{a1}^{ons} term, and the model is far more sensitive to this parameter than to all the other quantities discussed earlier. This phenomenologic parameter was estimated by matching with experimental data on the drop-out curves. In principle, one data point on a drop-out curve suffices to estimate this parameter value for a particular crude, and this value can be used for further predictions (other precipitants, effect of pressure, etc).

As we discussed before, several improvements and refinements can be made, but the model even in its present simple form captures the basic features of the liquid titration process and gives reasonable estimates of the amounts of solid precipitated by different diluents.

Pressure effect

The effect of pressure on the asphaltene precipitation was examined for a mixture of tank oil 2/propane (weight ratio 1:7) at 295 and 366 K (Hirshberg et al., 1984), and for fluid number 3 (live oil) at 373 K (Burke et al., 1990), Table 1. In agreement with the experimental observations, the asphaltene material precipitates as the pressure decreases.

For tank oil 2 with propane, all the asphaltene material precipitates as the pressure drops from 1,000 to 970 bar (we set $X_{a1}^{\text{ons}} = 9 \times 10^{-2}$ mole fraction). This is in line with the data, where the amount of precipitate at high pressures roughly corresponds to the asphaltene content of the crude. However, a more detailed comparison cannot be made, because resins were reported to coprecipitate with asphaltenes, whereas our model in its present form applies only to asphaltene precipitation.

A better comparison with the experimental data can be made for fluid number 3 (live oil). For this fluid we set $n = 500$, and $X_{a1}^{\text{ons}} = 5 \times 10^{-3}$ mole fraction, keeping all the other parameters the same as before. The crude is stable at high pressures, and in agreement with the experiment shows the asphaltene precipitation at about 275 bar (Figure 6). According to our model the precipitation upon depressurizing is, however, different from that in the liquid titration process. As the pressure decreases, the monomers are expelled from the petroleum fluid and there is no destruction of the micelles. The contribution of the lyophobic term becomes overwhelmingly important with the decrease of pressure. As a result, most of the asphaltene material remains in the crude in the form of micelles. At pressures below 208 bar (the calculated bubble point pressure, Table 2) the mixture is in a two-phase vapor-liquid region. We performed conventional vapor-liquid flash calculations at several pressures to obtain the composition of the liquid phase. This composition was the input for the asphaltene precipitation modeling. At pressures below 150 bar the liquid phase does not show any asphaltene precipitation. In the experiment, the ability of the crude to precipitate asphaltenes also reduces at lower pressures. Nevertheless, the model somewhat overestimates the effect of pressure (Figure 6).

Table 2. Bubble-Point Pressures of Petroleum Fluids

	Fluid Number*						
	3	4	6	7	8	9	10
T, K	373		3	7	6		333
p^{calc}, bar	208	38	75	148	218	135	257
p^{exp}, bar	201	41	71	157	255	134	248

*The numbers correspond to the following fluids: 3 = see Table 1; 4 = see Table 1; 6–8 = gas titration experiment, Burke et al., 1990; 6 = 80 mol % of mixture 4 + 20 mol % of gas mixture 5, see Table 1; 7 = 50 mol % of mixture 4 + 50 mol % of gas mixture 5; 8 = 30 mol % of mixture 4 + 70 mol % of gas mixture 5; 9 = Hirshberg et al., 1984, live oil No. 1 (corresponds to the tank oil No. 1, see Table 1); 10 = Hirshberg et al., 1984, live oil No. 2 (corresponds to the tank oil No. 2, see Table 1).

As was discussed earlier, the model predictions are sensitive to the resin content of the oil. There are no data on the resin content of fluid 3, and the amount of resin shown in Table 1 for this oil is arbitrary to a large extent. For instance, if we increase the resin amount of this oil 1.15 times (which corresponds to 10.3 mol % of resin), then there will be no precipitation at all in the pressure range shown in Figure 6 regardless of what value is assigned to X_{a1}^{ons} . Most of the available data on crude oil compositions do not report the resin content. We recommend resin content measurement for asphaltene precipitation studies.

Gas titration

The calculated precipitation curve and the experimental data by Burke et al. (1990) for gas titration are presented in Figure 7. Fluid 4 (Table 1) has been diluted with a gas titrant (mixture 5), as is explained in Table 2. The bubble-point pressures of the resulting fluids (mixtures 6, 7, 8) are also given in Table 2. The asphaltene precipitation was modeled at pressures above the saturation pressure. As before, we set $n = 500$; other parameters have the previous values except X_{a1}^{ons} . This latter parameter differs from crude to crude and has been set equal to 9×10^{-3} mole fraction. Figure 7 shows there is qualitative agreement between the data and the calculated results. The model predicts that at high solvent ratios the asphaltene material does not precipitate. The model also predicts, in agreement with the data, that when precipitation takes place, most of the asphaltene material still remains in the crude.

Concluding Remarks

The simple model proposed in this work can describe asphaltene stability and precipitation from crude mixtures. The model captures the basic features of the behavior of asphaltene-containing petroleum fluids. It predicts the change in the precipitation power of different alkane precipitants with their molecular weight. It gives the proper amount of precipitated asphaltene in liquid titration experiments and allows one to estimate the effect of pressure on asphaltene precipitation.

The model could be improved by relaxing some of the assumptions. Micellar size could be allowed to vary with pressure, temperature, and composition. More physically sound EOS could be used for the description of the bulk-crude phase, instead of the PR-EOS. The interaction between micelles could be taken into account in different ways

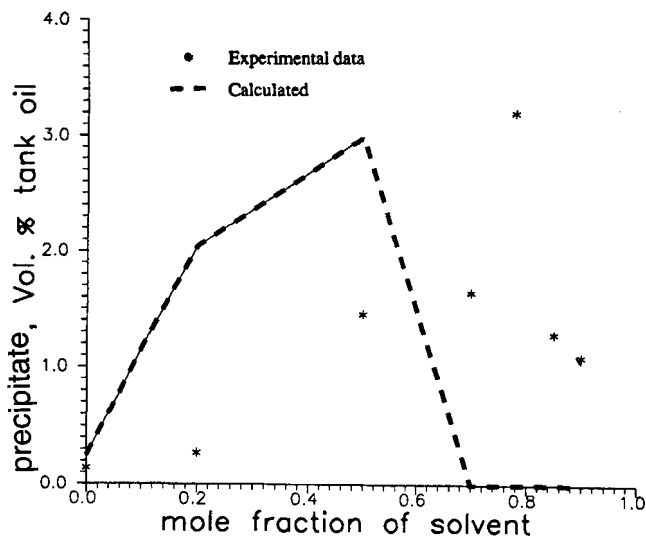


Figure 7. Effect of solvent content on precipitation curve for live oil 4 (Table 1) at 376 K.

(Blankstein et al., 1985; Chiew et al., 1995), and the osmotic pressure effect could be included. The effect of electrical charges could also be incorporated in the model to interpret recent conductivity measurements of asphaltene precipitation.

On the other hand, more experimental information is needed to further validate the model and remove the uncertainties in some of its parameter values. More detailed compositional measurements on petroleum fluids are necessary for reliable predictions. First, the amount of resin and asphaltene material in the crude should be measured. Their relative amounts determine the colloid stability. Reliable data on the molecular weight of asphaltene and resin monomers are also required. Data on asphaltene and resin molecular geometry would be very useful. Experimental information on asphaltene phase/petroleum fluid interfacial tension as well as on the heat of the adsorption of resins on asphaltene solids would be of value to provide micellization parameters.

Acknowledgments

We thank Norsk Hydro, Saudi Aramco, and Texaco for their support of this project. The authors are also thankful to Mr. Carlos Lira-Galeana for helpful discussions and for providing the software to carry out petroleum fluids characterization and bubble-point calculations.

Notation

k = Boltzmann constant
 N_i = number of moles of species i
 R = gas constant
 T = temperature
 X_i = mole fraction of species i

Literature Cited

- Altgelt, K. H., and M. M. Boduszynski, *Composition and Analysis of Heavy Petroleum Fractions*, Marcel Dekker, New York (1994).
- Andersen, S. I., and J. G. Speight, "Observations on the Critical Micelle Concentration of Asphaltenes," *Fuel*, **72**, 1343 (1993).
- Blankstein, D., G. M. Thurston, and G. Benedek, "Theory of Phase Separation in Micellar Solutions," *Phys. Rev. Lett.*, **54**(9), 955 (1985).

- Burke, N. E., R. E. Hobbs, and S. F. Kashou, "Measurement and Modeling of Asphaltene Precipitation," *J. Pet. Techn.*, 1440 (1990).
- Cavett, R. H., "Physical Data for Distillation Calculations, Vapor-Liquid Equilibria," Proc. Midyear Meeting, API Div. of Refining, San Francisco (May 15, 1964).
- Chiew, Y. C., D. Kuehner, H. W. Blanch, and J. M. Prausnitz, "Molecular Thermodynamics for Salt-Induced Protein Precipitation," *AIChE J.*, **41**, 2150 (1995).
- Cotterman, R. L., and J. M. Prausnitz, "Phase Equilibria for Mixtures Containing Very Heavy Components. Development and Application of Continuous Thermodynamics for Chemical Process Design," *Ind. Eng. Chem. Proc. Des. Dev.*, **24**, 194 (1985).
- Edmister, W. C., "Compressibility Factors and Equation of State," *Pet. Refiner*, **37**(4), 173 (1958).
- Espinat, D., and J. C. Ravey, "Colloidal Structure of Asphaltene Solutions and Heavy-Oil Fractions Studied by Small-Angle Neutron and X-Ray Scattering," *Int. Symp. Oilfield Chemistry*, SPE 25187, New Orleans (Mar. 2-5, 1993).
- Hirschberg, A., L. N. J. de Jong, B. A. Schipper, and J. G. Meijers, "Influence of Temperature and Pressure on Asphaltene Flocculation," *Soc. Pet. Eng. J.*, 283 (June, 1984).
- James, N., and A. K. Mehrotra, "V-L-S Multiphase Equilibrium in Bitumen-Diluent Systems," *Can. J. Chem. Eng.*, **66**, 870 (1988).
- Kahlweit, M., and H. Reiss, "On the Stability of Microemulsions," *Langmuir*, **7**, 2928 (1991).
- Katz, D. L., and K. E. Beu, "Nature of Asphaltic Substances," *Ind. Eng. Chem.*, **37**, 195 (1945).
- Katz, D. L., and A. Firoozabadi, "Predicting Phase Behavior of Condensate/Crude-Oil Systems Using Methane Interaction Coefficients," *J. Pet. Techn.*, 1649 (Nov., 1978).
- Kawanaka, S., S. J. Park, and G. A. Mansoori, "Organic Deposition From Reservoir Fluids: A Thermodynamic Predictive Technique," *SPE Reservoir Eng.*, 185 (1991).
- Leontaritis, K. J., "Asphaltene Deposition: A Thermodynamic-Colloidal Model," PhD Thesis, Univ. of Illinois, Chicago (1988).
- Leontaritis, K. J., and G. A. Mansoori, "Asphaltene Flocculation During Oil Production and Processing: A Thermodynamic Colloidal Model," SPE 16258, *SPE Int. Symp. Oilfield Chemistry*, San Antonio, TX (Feb. 4-6, 1987).
- Lian, H., J.-R. Lin, and T. F. Yen, "Peptization Studies of Asphaltene and Solubility Parameter Spectra," *Fuel*, **73**, 423 (1994).
- Mahadevan, H., and C. K. Hall, "Statistical-Mechanical Model of Protein Precipitation by Nonionic Polymer," *AIChE J.*, **36**(10), 1517 (1990).
- McBain, M. E., and E. Hutchinson, *Solubilization and Related Phenomena*, Academic Press, New York (1955).
- Nagarajan, R., and E. Ruckenstein, "Theory of Surfactant Self-Assembly: A Predictive Molecular Thermodynamic Approach," *Langmuir*, **7**, 2934 (1991).
- Nellensteyn, F. I., "The Colloidal Structure of Bitumens," *The Science of Petroleum*, Vol. 4, Oxford Univ. Press, London, p. 2760 (1938).
- Peng, D.-Y., and D. B. Robinson, "A New Two-Constant Equation of State," *Ind. Eng. Chem. Fundam.*, **15**, 59 (1976).
- Prigogine, I., and R. Defay, *Chemical Thermodynamics*, Longmans, Green, New York (1952).
- Puvvada, S., and D. Blankstein, "Thermodynamic Description of Micellization, Phase Behavior, and Phase Separation of Aqueous Solutions of Surfactant Mixtures," *J. Phys. Chem.*, **96**, 5567 (1992).
- Rusanov, A. I., *Micelle Formation in Surfactant Solutions*, in Russian, Chimia, St. Petersburg (1992).
- Speight, J. G., *The Chemistry and Technology of Petroleum*, Marcel Dekker, New York (1980).
- Storm, D. A., R. J. Barresi, and S. J. DeCanio, "Colloidal Nature of Vacuum Residue," *Fuel*, **70**, 779 (1991).
- Storm, D. A., and E. Y. Sheu, "Characterization of the Asphaltic Colloidal Particle in Heavy Oil," Eastern Oil Shale Symp., Institute for Mining and Minerals Research, Univ. of Kentucky, Lexington (Nov. 16-19, 1993).
- Storm, D. A., E. Y. Sheu, and M. M. De Tar, "Macrostructure of Asphaltenes in Vacuum Residue by Small-Angle X-ray Scattering," *Fuel*, **72**, 977 (1993).
- Storm, D. A., and E. Y. Sheu, "Evidence for Micelle-Like Asphaltenes in Crude Oil," Colloid and Surface Science Symp. Amer. Chem. Soc., Stanford, CA (June 19-22, 1994).
- Tanford, C., *Hydrophobic Effect: Formation of Micelles and Biological Membranes*, Wiley, New York (1973).
- Vlachy, V., H. W. Blanch, and J. M. Prausnitz, "Liquid-Liquid Phase Separations in Aqueous Solutions of Globular Proteins," *AIChE J.*, **39**(2), 215 (1993).
- Whitson, C. H., "Characterizing Hydrocarbon Plus Fractions," *Soc. Petrol. Eng. J.*, 683 (Aug., 1983).
- Wiehe, L. A., and K. S. Liang, "Asphaltenes, Resins, and Other Petroleum Macromolecules," *Int. Conf. Fluid Properties and Phase Equilibria for Chemical Process Design*, Snowmass, CO (June 18-23, 1995).
- Yen, T. F., "Structure of Petroleum Asphaltene and Its Significance," *Energy Sources*, **1**, 447 (1974).

Appendix A: Derivation of Eq. 26

From Eq. 7 one can write:

$$\ln X_M = n_1 \ln X_{a1} + n_2 \ln X_{r1} + \Delta G_M^{00}/kT, \quad (A1)$$

where the last term can be calculated from Eq. 23. The next step is to perform differentiation in Eq. 25; it is more convenient to use (n, Θ) variables than (n_1, n_2) . The relationships between these variables are given by

$$\Theta = \frac{A_r(n_2)}{A_\Sigma(n_1)} = \frac{n_2}{n_1 b + n_2^s}, \quad \text{and} \quad n = n_1 + n_2, \quad (A2)$$

where b is given in Eq. 27. From the preceding equations:

$$n_1 = \frac{n - n_2^s \Theta}{1 + b \Theta}, \quad (A3)$$

$$n_2 = \frac{nb + n_2^s}{1 + b \Theta} \Theta. \quad (A4)$$

To find how n_2^s and b change with Θ , one needs a detailed knowledge of the geometry of an asphaltene molecule and how it is accommodated within a micelle. Since such information is not currently available, one simple approach is to assume that b and n_2^s do not depend on coverage fraction, Θ , at constant n (for our model, this assumption implies that the micellar radius, Eq. 17, does not change with coverage fraction). One can then proceed to calculate

$$\left(\frac{\partial n_1}{\partial \Theta} \right)_n = - \frac{1}{nb + n_2^s} \left(\frac{n_2}{\Theta} \right)^2 \quad (A5)$$

$$\left(\frac{\partial n_2}{\partial \Theta} \right)_n = \frac{1}{nb + n_2^s} \left(\frac{n_2}{\Theta} \right)^2. \quad (A6)$$

Combining Eqs. A1, 23-25, A5, and A6 results in Eq. 26 of the text.

Appendix B: Characterization of Petroleum Fluids

The three-parameter gamma-distribution (Whitson, 1983) was used to describe the C_{7+} residue and a quadrature technique (Cotterman and Prausnitz, 1985) was used to perform lumping. The C_{7+} residue was represented by 3 to 5 pseudo-components (ps-1, ps-2, etc.). In this procedure, the asphaltenes were excluded from the C_{7+} residue, and the resins

Table A1. Acentric Factors, Critical Temperatures and Critical Pressures of Heavy Ends of Petroleum Fluid Mixtures

Heavy Ends	Fluid Number*											
	ω	1 T_c, K	P_c, bar	ω	2 T_c, K	P_c, bar	ω	3 T_c, K	P_c, bar	ω	4 T_c, K	P_c, bar
ps-1	0.630	629.2	24.0	0.553	601.1	26.1	0.590	614.7	25.1	0.540	596.2	26.5
ps-2	0.948	729.0	16.6	0.706	655.8	22.1	1.064	757.2	14.7	0.889	713.0	17.8
ps-3	1.20	942.4	8.5	0.917	720.9	17.2	1.322	806.5	11.7	1.074	759.4	14.5
ps-4	—	—	—	1.286	800.4	12.0	—	—	—	1.580	846.1	10.0
ps-5	—	—	—	1.35	951.1	8.5	—	—	—	—	—	—
Resin	1.4	917.5	8.6	1.4	917.5	8.6	1.4	917.5	8.6	1.4	917.5	8.6
Asphalt	1.8	1,003	8.8	1.8	1,003	8.8	1.8	1,003	8.8	1.8	1,003	8.8

*See Table 1.

were introduced by dividing the heaviest pseudocomponent into two; resins of a predetermined molecular weight, and the remainder of the heaviest pseudocomponent. The results of the characterization are shown in Table 1. The Cavett (1964) correlation was then used to obtain critical properties of the PR-EOS. The acentric factors of the very heavy ends of the crudes have been assigned the following values: 1.8 for the asphaltenes; 1.4 for the resins. These and other values of acentric factors (Edmister, 1958) provide reasonable calculated bubblepoint pressure (Table 2). The latter were computed from the PR-EOS for liquid compositions obtained by taking into account the micellization equilibrium in the crude. The values of acentric factors, critical pressures, and critical

temperatures for the heavy ends of various fluid mixture of Table 1 are given in Table A1.

Methane interaction coefficients for the PR-EOS were from Katz and Firoozabadi (1978) using the molecular weight rather than density correlation. The interaction coefficients of asphaltenes with the other components of the crude were assigned the following values: 0.15 (C_1), 0.11 (C_2), 0.09 (C_3), 0.05 (C_4), 0.04 (C_5), 0.02 (C_6), 0.01 (C_8 to C_{12}), and zero with the heavier fractions. The resin interaction coefficients were set to zero.

Manuscript received Feb. 14, 1995, and revision received Sept. 18, 1995.